Berberine Targets Assembly of *Escherichia coli* Cell Division Protein FtsZ†

Prerna N. Domadia,‡,§ Anirban Bhunia,|| J. Sivaraman,⊥ Sanjay Swarup,*,⊥ and Debjani Dasgupta*,‡

Department of Biochemistry, The Institute of Science, Mumbai 400 032, India, Department of Biological Sciences, National University of Singapore, Singapore 117543, and School of Biological Sciences, Nanyang Technological University, Singapore 637551

Received September 11, 2007; Revised Manuscript Received January 9, 2008

ABSTRACT: The ever increasing problem of antibiotic resistance necessitates a search for new drug molecules that would target novel proteins in the prokaryotic system. FtsZ is one such target protein involved in the bacterial cell division machinery. In this study, we have shown that berberine, a natural plant alkaloid, targets *Escherichia coli* FtsZ, inhibits the assembly kinetics of the Z-ring, and perturbs cytokinesis. It also destabilizes FtsZ protofilaments and inhibits the FtsZ GTPase activity. Saturation transfer difference NMR spectroscopy of the FtsZ−berberine complex revealed that the dimethoxy groups, isoquinoline nucleus, and benzodioxolo ring of berberine are intimately involved in the interaction with FtsZ. Berberine perturbs the Z-ring morphology by disturbing its typical midcell localization and reduces the frequency of Z-rings per unit cell length to half. Berberine binds FtsZ with high affinity ($K_D \sim 0.023$ μM) and displaces bis-ANS, suggesting that it may bind FtsZ in a hydrophobic pocket. Isothermal titration calorimetry suggests that the FtsZ−berberine interaction occurs spontaneously and is enthalpy/entropy-driven. *In silico* molecular modeling suggests that the rearrangement of the side chains of the hydrophobic residues in the GTP binding pocket may facilitate the binding of the berberine to FtsZ and lead to inhibition of the association between FtsZ monomers. Together, these results clearly indicate the inhibitory role of berberine on the assembly function of FtsZ, establishing it as a novel FtsZ inhibitor that halts the first stage in bacterial cell division.

FtsZ[1] is an ancestral homologue of tubulin, signifying a universal role in prokaryotic cell division (*1*). In the early stage of bacterial cytokinesis, FtsZ, a GTPase, polymerizes at the division site to form a dynamic Z-ring around the inner circumference (*2*). Identification of novel anti-FtsZ agents that would prevent cell division by disrupting Z-ring formation can overcome the crisis of drug resistance and lead to new antibacterial drug discovery. In recent years, a fair number of natural as well as synthetic small molecule inhibitors have been identified to perturb the Z-ring assembly in *Escherichia coli*, *Mycobacterium tuberculosis*, *Bacillus subtilis*, or *Pseudomonas aeroginosa* FtsZ (*3–17*). Among the naturally derived FtsZ inhibitors, a few do not inhibit Gram-negative bacteria (*5–7*) whereas others are cytotoxic (*8*) or unstable (*9*). The antibacterial spectrum of some synthetic FtsZ inhibitors (*10–13*) still needs to be identified. In continuation of our search (*9*) toward newer, safer, naturally occurring small molecule FtsZ inhibitors with a broad spectrum of antibacterial activity, we report the identification of berberine, a benzylisoquinoline alkaloid, as a potential inhibitor of FtsZ polymer dynamics *in vivo* and perhaps as a modulator of bacterial cytokinesis.

Berberine is a natural plant product obtained from various species of *Berberis* such as *Berberis aquifolium* and *Berberis aristata*. In aqueous solution, berberine exists as the quaternary ammonium base 9,10-dimethoxy-5,6-dihydro[1,3]dioxolo[4,5-*g*]isoquino[3,2-*a*]isoquinoline-7-ilium (IUPAC nomenclature). Plants containing berberine have been traditionally used in Chinese and Native American medicine to fight a number of infectious organisms, and the sulfate, hydrochloride, and chloride forms are used in Western pharmaceutical medicine as antibacterial agents (*18*). It exhibits antimicrobial activity against a variety of bacteria, fungi, protozoans, helminthes, chlamydia, and viruses (*19–21*). Interestingly, berberine inhibits the overgrowth organisms such as staphylococci, coliforms, and yeasts without affecting indigenous lactobacilli and bifidobacteria (*22*). Moreover, it is active against pathogenic Gram-positive and Gram-negative bacteria such as *Bacillus pumilus*, *Bacillus cereus*, *B. subtilis*, *Corynebacteriom diphtheriae*, *Shigella boydii*, *E. coli*, *Klebsiella pneumoniae*, *Cryptococcus neoformans*, *Staphylococcus aureus*, *Symphoricarpos albus*, *Streptococcus*

† J.S. and S.S. were funded by Research Grants R154-000-245-112 and R-154-000-290-112 from the Academic Research Fund (ARF), National University of Singapore (NUS), respectively. D.D. was funded by Grant 37/47/BRNS/2291 from Department of Atomic Energy (Government of India). This work was supported from the above funds.

* Address correspondence to these authors. D.D.: tel, +9122 22844219(ext 501); fax, +91 22871639; e-mail, drdasgupta88@rediffmail.com. S.S.: tel, +65 65167993; e-mail, dbsss@nus.edu.sg.

‡ The Institute of Science.

§ Present address: School of Medicine, Juntendo University, Tokyo 113-8421, Japan.

|| Nanyang Technological University.

⊥ National University of Singapore.

[1] Abbreviations: FtsZ, filamentation temperature sensitive protein Z; GTP, guanosine 5-triphosphate; MES, 2-morpholinoethanesulfonic acid; TNP-GTP, 2′- (or 3′-) *O*-(trinitrophenyl) guanosine 5′-triphosphate; GFP, green fluorescent protein; STD NMR, saturation transfer difference nuclear magnetic resonance; bis-ANS, 4,4′-dianilino-1,1′-binaphthalene-5,5′-disulfonic acid; MIC, minimum inhibitory concentration; MRSA, methicillin-resistant *Staphylococcus aureus*; FPLC, fast protein liquid chromatography; ITC, isothermal titration calorimetry; T7, tubulin-like loop 7.

10.1021/bi7018546 CCC: $40.75 © 2008 American Chemical Society
Published on Web 02/15/2008

pyogenes, *Streptococcus mutans*, *Vibrio cholerae*, and *Clostridium perfringes* (*23, 24*). Berberine is active against multiple drug-resistant *M. tuberculosis* (*25*) and methicillin-resistant *S. aureus* (*26*). Despite much information on the antimicrobial potential of berberine, the actual mechanism for inhibition of bacteria has not yet been established. The aim of this study was to understand the role of berberine as an inhibitor of FtsZ assembly dynamics in *E. coli* using biochemical assays, electron and confocal imaging, modeling, NMR and fluorescence spectroscopy, and isothermal titration calorimetry. In the future, the functional elucidation of berberine and other structurally related FtsZ inhibitors such as sanguinarine (*8*) can allow rational designing of their derivatives, leading to the development of specific analogues with anti-FtsZ activity.

MATERIALS AND METHODS

Materials. GTP, MES, LB, Tris-HCl, KCl, and $MgCl_2$ were purchased from Sigma (St. Louis, MO). Bis-ANS and IPTG were purchased from Molecular Probes (Johnson City, OR). Berberine sulfate was obtained from BDH Chemicals (Poole, England). Nickel resin was from Qiagen (Chatsworth, CA). Deuterium oxide was from Cambridge Isotope Laboratories (Andover, MA). All other chemicals were of analytical grade.

FtsZ Purification. Wild-type FtsZ was purified from the recombinant *E. coli* K-12 strain (*9, 27*) using nickel−NTA affinity chromatography. Its homogeneity was further verified using dynamic light scattering (DynaPro Protein Solutions, Santa Barbara, CA), native PAGE, and gel filtration (AKTA FPLC; GE Healthcare Ltd., Little Chalfont, U.K.).

Light-Scattering Assay. A standard GTP initiated *in vitro* light-scattering assay (*28*) was performed. Real-time detection of polymerization of FtsZ at 12.5 μM was monitored on a LS-55 fluorescence spectrometer (Perkin-Elmer Corp., Waltham, MA) in the absence and presence of berberine up to 200 μM.

GTP Hydrolysis Assay. A standard malachite green sodium molybdate assay (*29*) was done to quantify GTP hydrolysis during FtsZ assembly in the presence of berberine (0–200 μM).

Electron Microscopy. Untagged-wild-type FtsZ at 12.5 μM was polymerized in assembly buffer for 10 min. One hundred micromolar berberine was added to the FtsZ protofilaments. Samples were prepared for electron microscopy (*9*), and images were collected at 50000× magnification using a CM 200 transmission electron microscope (Philips Electron Optics, FEI Co., Portland, OR).

STD NMR Spectroscopy. The exchangeable protons of FtsZ were exchanged into deuterated buffer: 50 mM sodium phosphate buffer (pH 6.5, uncorrected due to deuterium effects), 50 mM NaCl, and 5 mM $MgCl_2$. As described earlier (*9*), 1D STD NMR spectra of 15 μM FtsZ and 1500 μM berberine complex were recorded on a Bruker Avance DRX 600 spectrometer equipped with a cryoprobe at 298 K using the standard STD NMR pulse sequence (*30*) and WATERGATE 3-9-19 sequence for water suppression. FtsZ signals were suppressed using 15 kHz of a spin-lock pulse for 20 ms. Selective irradiation of FtsZ was achieved by a train of Gaussian-shaped pulses with a 1% truncation and each of 49 ms in duration and separated by a 1 ms delay. A total of 40 selected pulses were applied, leading to a total time of saturation to 2 s. The so-called on resonance for FtsZ was in the aliphatic region of the spectrum at a frequency of 0.15 ppm, and off resonance was at 40 ppm, where neither FtsZ nor the berberine resonances were present. Subtraction of the two spectra (on resonance − off resonance) by phase cycling resulted in a difference spectrum that contained signals arising from the saturation transfer. The numbers of scans for reference and difference spectra were 256 and 512, respectively. Data processing was done using the TopSpin program (Bruker Biospin Corp., Billerica, MA). The H3 proton of berberine showed the strongest STD effect so, based on the principle of group epitope mapping (*31*), its value was set to 100%, and all other proton intensities were calculated with respect to this group.

Isothermal Titration Calorimetry (ITC). ITC titrations of 10 μM FtsZ with 25 μM berberine, dialyzed in 50 mM MES, pH 6.8, 50 mM KCl, and 5 mM $MgCl_2$, were performed on a VP-ITC microcalorimeter (Micro Cal Inc., Northampton, MA). FtsZ (volume ~1.43 mL) was titrated with 50 injections of berberine (5 μL per injection) at 3 min intervals. The data were analyzed using Origin 5.0 (Micro Cal Inc.).

Fluorescence Spectroscopy. To study the binding of FtsZ to berberine, 10 μM berberine was treated with increasing doses of FtsZ (2–20 μM) in 10 mM Tris buffer, pH 7.4. To probe the displacement of berberine from FtsZ, fluorescence spectral changes of the FtsZ−berberine complex (1:10 molar ratio) at 530 nm, as a function of increasing doses of GTP (50−500 μM), were probed on a LS 55 spectrofluorometer (Perkin-Elmer Corp.). Samples were excited at 430 nm to measure the intrinsic berberine fluorescence at 550 nm emission (*32*). Similarly, to probe the displacement of berberine from FtsZ, fluorescence spectral changes of the FtsZ-bound TNP-GTP (1:10 molar ratio) at 540 nm, as a function of increasing doses of berberine (100−500 μM), were probed by exciting the fluorescent-labeled TNP-GTP at 410 nm (*33*). Fluorescence spectra were acquired using a LS 55 spectrofluorometer. Further, to probe the displacement of bis-ANS by berberine, the FtsZ (12.5 μM)−bis-ANS (10 μM) complex was treated with different doses of berberine and excited at 390 nm, and the emission was recorded at 494 nm (*4*).

Confocal Imaging. E. coli cells expressing the FtsZ−GFP fusion were grown to prelogarithmic phase and treated with 100 μM berberine for 1 h before visualizing by a LSM 510 Meta confocal laser scanning microscope (Carl Zeiss Micro Imaging GmbH, Bernried, Germany) with a 63× oil objective and GFP filter at 488 nm. Analysis was done using the ImageJ program (National Institutes of Health, Bethesda, MD).

Molecular Modeling. Using AutoDock 3.0 (*34*), the three-dimensional coordinates of berberine were docked into a 3D homology model of the *E. coli* FtsZ structure, built in this study from the crystal structure of *Methanococcus jannaschii* (PDB code 1FSZ) (*35*). In brief, grid maps (grid spacing, 0.375 Å) were constructed using 127 × 127 × 127 points and Kollmann atom charges employed by Sybyl 7.1 (Tripos Inc., St. Louis, MO). A total of 250 Lamarckian genetic algorithm runs were performed. From binding modes clustered using an rmsd of 1.0 Å, the resultant cluster with the lowest docking energy was considered.

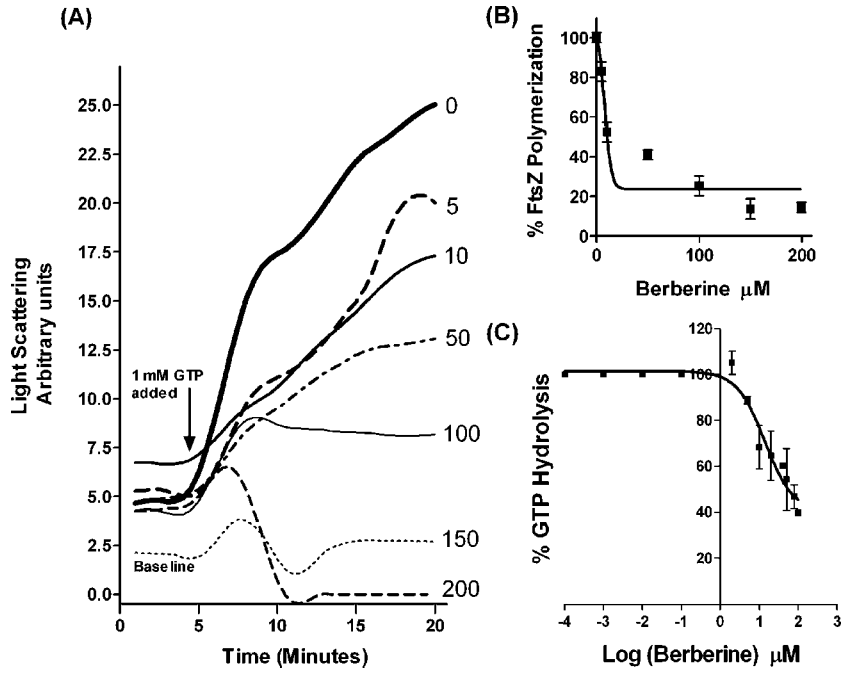

FIGURE 1: Kinetics of FtsZ assembly and GTPase inhibition by berberine. (A) FtsZ polymerization in 0, 5, 10, 50, 100, 150, and 200 μM berberine at pH 6.5 in assembly buffer, as initiated by 1 mM GTP. The line patterns are indicated in the figure itself. (B) IC_{50} for berberine. 10.0 $\pm$ 2.5 μM is shown. (C) GTP hydrolysis at 37 °C for 15 min in the presence of different doses of berberine (5–100 μM).

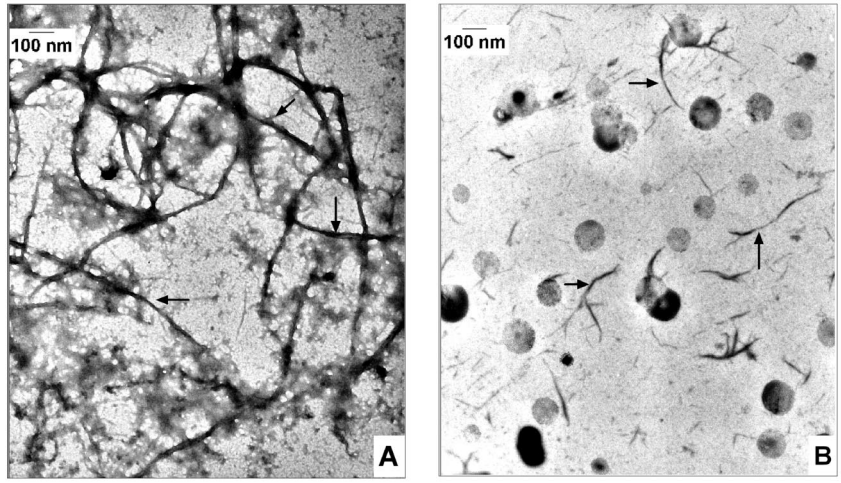

FIGURE 2: Electron microscopy of FtsZ protofilaments. (A) Electron micrograph of the polymerized network of FtsZ. (B) Reduction of FtsZ bundles when treated with 100 μM berberine. Black arrows in both panels show FtsZ protofilaments.

RESULTS

Berberine Inhibits the FtsZ Assembly and GTPase Activity. An increase in light scattering at 340 nm is a semiquantitative measure for the rate of real-time FtsZ assembly kinetics *in vitro* (*28*). Berberine inhibited the light-scattering signal of the FtsZ assembly in a dose-dependent manner (Figure 1A). GTP-initiated FtsZ polymerization was inhibited by 85%, 75%, 59%, 47%, and 17% with 200, 100, 50, 10, and 5 μM berberine, respectively. The plot of berberine-dependent FtsZ assembly after 15 min shows an IC_{50} of 10.0 $\pm$ 2.5 μM (Figure 1B).

The assembly of FtsZ is dependent on the rate of GTP hydrolysis (*1, 36*). Here, the inhibitory activity of berberine was directly related to a reduction in the rate of GTP hydrolysis during the FtsZ assembly process. Berberine at 5, 20, and 100 μM suppresses the rate of GTP hydrolysis of FtsZ monitored for 15 min by 12%, 46%, and 60%, respectively. Thus, berberine significantly inhibited the FtsZ GTPase activity in a dose-dependent manner with an IC_{50} of 16.01 $\pm$ 5.0 μM (Figure 1C), which affected the stability of the FtsZ polymers. Electron microscopy further verified that FtsZ protofilaments were destabilized by berberine. An extensive network of long, straight GTP-bound, FtsZ protofilaments of a higher assembly order was observed in the presence of 1 mM GTP (Figure 2A). Addition of 100 μM berberine to preformed wild-type FtsZ−GTP protofilaments (Figure 2B) resulted in a few thin, short, curved filaments of FtsZ and dot-like FtsZ monomeric structures, which confirmed that berberine inhibited FtsZ assembly by weakening its self-association process.

Group Epitope Mapping of Berberine in the Presence of FtsZ. The STD NMR technique is used to characterize

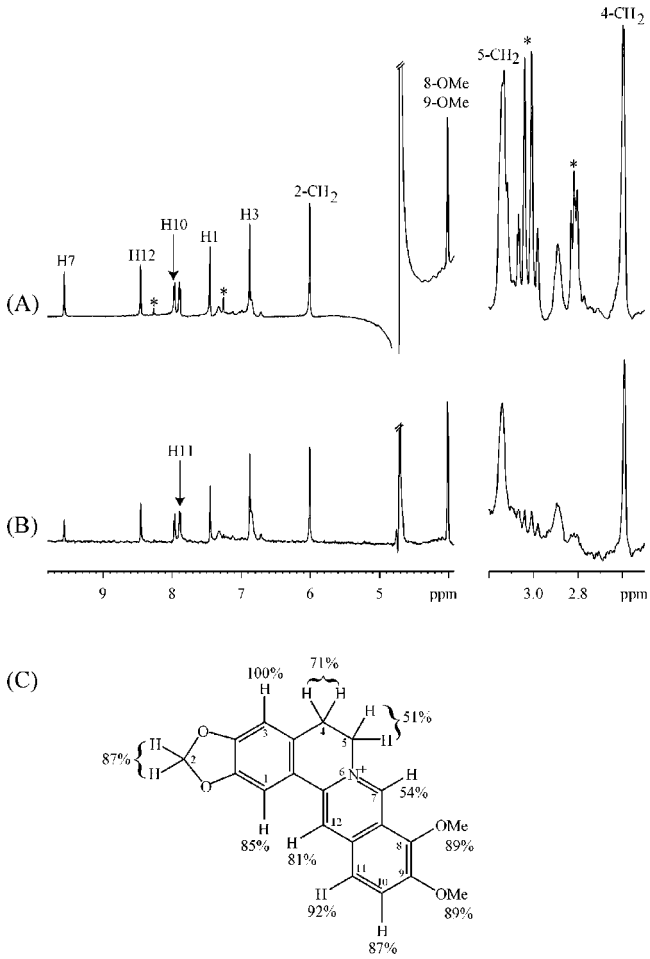

FIGURE 3: STD NMR spectra and group epitope mapping. (A) Reference STD NMR spectrum. (B) STD NMR spectra of berberine in the presence of FtsZ showing peaks only for bound berberine. Asterisks indicate the signals from impurities in the buffer, which do not bind to FtsZ. (C) Group epitope mapping of berberine from ^{1}H STD NMR spectra. Higher percent of berberine protons indicates a closer proximity to the surface of FtsZ.

binding and identify epitopes of the ligand that bind to a protein receptor (*30, 31*). Here, STD NMR was used to map the binding epitopes of berberine in close proximity to the FtsZ surface, involved in the binding process (Figure 3). Since the saturation transfer from the protein (FtsZ) to the ligand (berberine) is fast (K_D = 0.023 μM), it indicates a "fast off-rate" of the ligand transferring the information about saturation from the protein–ligand complex into the solution. In the case of a fast off-rate, a large excess of ligand is used so that one binding site can be used to saturate many ligand molecules in a few seconds. Hence we used a 100-fold molar excess of berberine over FtsZ, as is well explained by the pioneers of STD NMR (*30, 31*). Selective irradiation of the signal from FtsZ (on resonance spectrum), nonoverlapping with the berberine signal, exclusively transfers the effective magnetization via spin diffusion from FtsZ to berberine. Subtraction of the above spectrum from a reference proton NMR spectrum in which the FtsZ is not saturated (Figure 3A) resulted in the difference spectrum (Figure 3B), which contains only signals of berberine, with low molecular weight impurities being removed. The relative degrees of saturation for the individual protons of berberine are displayed in Figure 3C. The H1, 2-CH_2, H3, H10, H11, H12, and methyl group

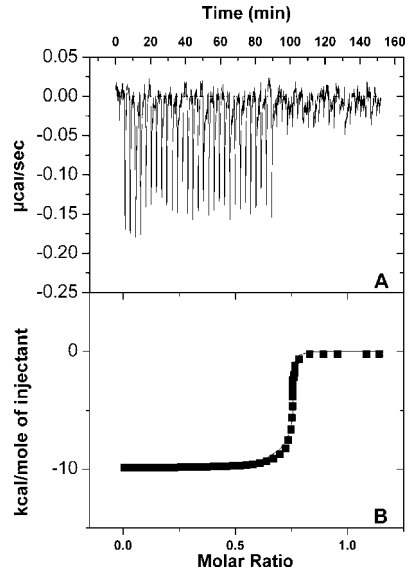

FIGURE 4: Thermodynamics of binding between FtsZ and berberine. (A) Plot of rate of heat released as a function of time by titrating berberine (25 μM) to FtsZ (10 μM) in 50 mM MES, 50 mM KCl, and 5 mM $MgCl_2$, pH 6.8 at 20 °C. (B) Plot of exchange of heat per mole of injectant versus molar ratio of berberine, after subtraction of buffer control.

(8-OMe or 9-OMe) protons have STD intensities between 80% and 100%. These positions, therefore, are in intimate contact with the FtsZ binding site. On the other hand, 4-CH_2 protons have medium STD intensities of 71%. In contrast, the lowest intensities correspond to H7 and 5-CH_2protons, which have intensities as low as 50%. Thus, a clear distinction was observed between berberine protons with a high or low affinity to FtsZ.

Thermodynamics of the Berberine−FtsZ Binding. ITC provides thermodynamic characterization of the specific molecular interactions associated with the binding reaction. Figure 4 shows the binding isotherm of FtsZ with 5 μL aliquots of berberine at 298 K, showing the heats released (microjoules) during FtsZ−berberine interactions (Figure 4 A), which were integrated and plotted as a function of the molar ratio of berberine (Figure 4B). On the basis of ITC data, various thermodynamic parameters were derived using one site binding model based on the Marquardt nonlinear regression (*37*). It yielded a binding stoichiometry of 1:1 for berberine to FtsZ and an equilibrium association constant (K_A) of 43.9 ± 9.75 × 10^6 M^{-1}. The dissociation constant (K_D) was calculated to be ~0.02 μM. The enthalpy change (ΔH) of the binding of berberine to FtsZ was −9.9 ± 1.35 kcal·mol^{-1}. The entropy change (ΔS) was found to be 1.2 cal·mol^{-1}·deg^{-1}. The binding free energy (ΔG) of berberine was calculated to be −10.4 ± 0.1 kcal·mol^{-1}.

Binding of Berberine to FtsZ Changes Its Spectral Characteristics. In aqueous buffers, berberine has an extremely weak intrinsic fluorescence emission spectrum with a λ_{max} at 550 nm (*38*). Upon formation of a complex with FtsZ, the fluorescence intensity of berberine increases 5-fold (Figure 5A). Moreover, a typical blue shift occurs in its emission maxima from 550 to 515 nm in response to FtsZ binding that affects the local environment around the aromatic ring in berberine. It further showed that saturation of 10 μM berberine was reached after addition of 10 μM FtsZ.

Berberine Binds in the Hydrophobic Pocket of FtsZ. Bis-ANS is a fluorescent dye that fluoresces strongly in hydro-

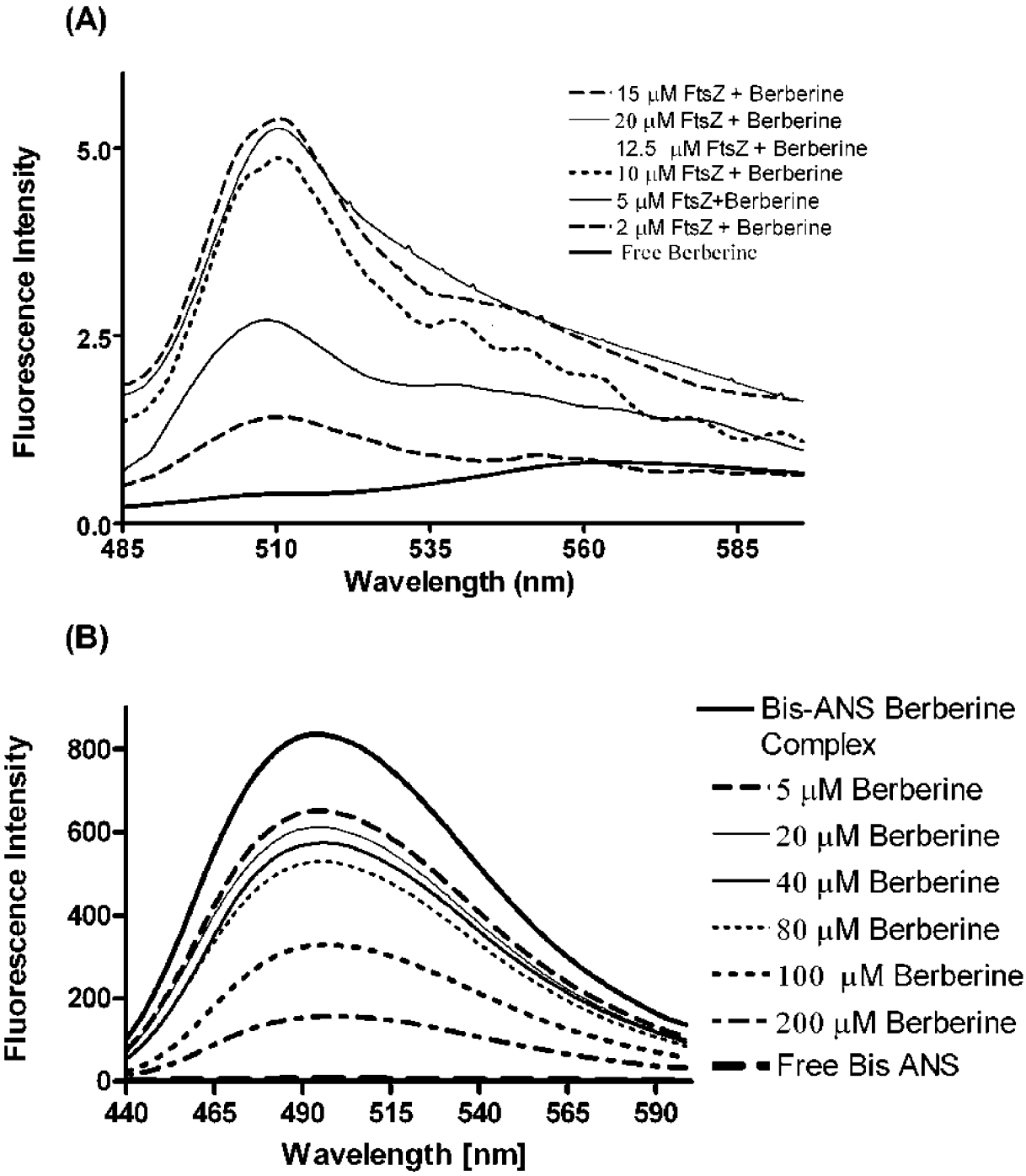

FIGURE 5: Fluorescence measurements. (A) Blue shift of the emission maxima of berberine on binding FtsZ in 10 mM Tris buffer, pH 7.4, Free berberine (10 μM) fluoresces at 550 nm, bound berberine fluoresces at 515 nm, shown at increasing concentrations of FtsZ: 2, 5, 10, 12.5, 15, and 20 μM. (B) Quenching of the bis-ANS−FtsZ complex by berberine at increasing concentrations, viz., 20, 40, 60, 80, 100, and 200 μM. The line patterns are indicated in the figure itself.

phobic environments and almost negligibly in water (*39*). Binding of bis-ANS to hydrophobic surfaces of FtsZ is signaled by a 800-fold increase in fluorescence intensity and blue shift of the emission maximum peak from 530 to 494 nm. Berberine further quenches this FtsZ−bis-ANS complex (Figure 5B) in a dose-dependent manner, indicating that binding of berberine to FtsZ displaces bis-ANS on FtsZ. It was previously reported (*4*) that bis-ANS binds to FtsZ in a hydrophobic region and inhibits FtsZ self-assembly through hydrophobic interactions of FtsZ. This indicates that berberine may also bind to FtsZ in a hydrophobic region probably involving the bis-ANS binding pocket. Furthermore, the inhibition of bis-ANS binding to FtsZ by berberine (Figure 5B), and vice versa (data not shown), suggests that the binding sites of berberine and bis-ANS may overlap.

The Berberine Binding Site Overlaps with the GTP Binding Pocket in FtsZ. Binding sites of GTP and bis-ANS overlap on FtsZ (*4*). It is quite likely that berberine may have high affinity for the hydrophobic region involved in the GTP binding site. We performed competitive assays between GTP and berberine using a fluorescence displacement experiment, as berberine possesses intrinsic fluorophoric groups like the aromatic ring and isoquinoline moiety. Sequential addition of increasing concentrations of GTP to the berberine-bound

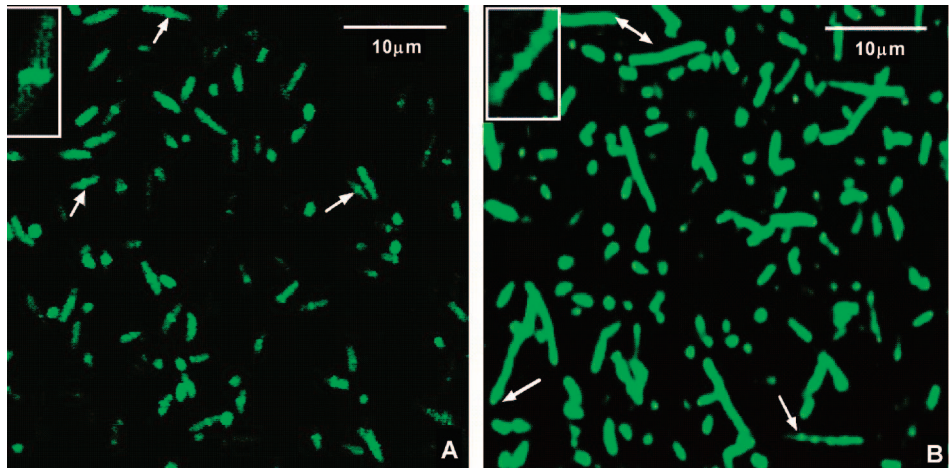

FIGURE 6: Spatial perturbation of the Z-ring by berberine. (A) Typical Z-ring patterns in control *E. coli* cells. (B) Spatial disorganization of the Z-ring pattern in cells treated with 100 μM berberine. White arrows in both panels show the respective characteristics of the Z-ring.

Table 1: Effects of Berberine on Z-Rings of *E. coli* Cells

E. coli Z rings	control	5 μM berberine	50 μM berberine	100 μM berberine
frequency of Z-rings per μM	5.00 ± 0.04	3.18 ± 0.13	2.94 ± 0.11	2.72 ± 0.13
% of cells having Z-rings[a]	85.70	78	51	36

[a] 100 cells were analyzed to calculate the frequency of Z-rings.

FtsZ complex leads to a consistent dose-dependent decrease in fluorescence intensity of the complex (Figure 1A, Supporting Information). This implies that the berberine and GTP binding sites probably overlap such that subtle conformational changes in the GTP binding pocket affect the binding of berberine to FtsZ.

Further, we also used TNP-GTP to monitor the effect of berberine on the GTP binding site on FtsZ. TNP-GTP is a trinitrophenylated fluorescent analogue of GTP and is known to bind to FtsZ (*40*). The fluorescence intensity of the TNP-GTP-bound FtsZ complex at 540 nm was not found to change upon addition of berberine up to 500 μM (Figure 1B, Supporting Information). This suggests that berberine cannot compete with GTP for its binding site on FtsZ.

Berberine Perturbs Z-Ring Formation in Vivo. A GFP tag on FtsZ allows dynamic tracking of FtsZ movement and turnover and elucidates the inhibitory role of berberine in live *E. coli* cells (*41*). Here, the true dynamics of the Z-ring conformation could be seen in *E. coli* cells which were not treated chemically for fixation. In the absence of berberine, typical structures of fluorescent Z-rings localized at the midcell of dividing cells were visualized by confocal imaging (Figure 6A). Treatment with 100 μM berberine for 75 min changed the spatial characteristics, midcell position, and frequency of Z-rings in numerous cells (Figure 6B). A typical phenotype for cell division inhibition with nearly doubled cell length was observed. Berberine-treated cells have a mean length of 6.95 μm as compared to the mean length of 3.45 μm for control cells. Berberine perturbed the formation of typical Z-ring morphology *in vivo*, reduced the occurrence of Z-rings from 85.7% (0 μM) to 36% (100 μM) (Table 1), and halted the septation process. Thus, berberine showed a 3-fold effect; it blocked FtsZ assembly, interfered with the Z-ring assembly, and inhibited cell division.

Docking Studies. In silico docking simulations using AutoDock 3.0 predicts the bound conformations of a small molecule ligand to a nonflexible macromolecular target of known structure (*34*). So far, the structure of *E. coli* FtsZ (Swiss-Prot ID P06138) employed in this study is not known. Hence, a predicted 3D structure of FtsZ for *E. coli* constructed by homology modeling was used for docking the ligand berberine onto a rigid molecule of FtsZ. The docked conformations generated by 250 independent runs readily placed berberine within the binding pocket of GTP, in a low-energy orientation characterized with optimal hydrophobic side chain interactions, viewed by PyMOL (Figure 7B,D). The putative binding site proposed by AutoDock correlates well with the STD NMR data. In the proposed model, Thr 132, Pro 134, Phe 135, Ile 163, Pro 164, Phe 182, and Leu 189, which are in close proximity to the binding epitopes of berberine, are speculated to interact, mainly through hydrophobic interactions (Figure 7C). Further, we have provided detailed calculations showing the interproton distances between FtsZ and berberine based on the *in silico* docking model (Table 1, Supporting Information), which precisely explains that the 5-CH_2 and H7 protons of berberine are far in distance from the FtsZ protons in comparison to other protons of the berberine.

DISCUSSION

Currently, only a few of the known antibacterial agents act by targeting the bacterial cell division process via FtsZ, which is a highly conserved constituent and a fundamental component of the cell division machinery. This makes FtsZ a promising target for drugs with a novel mode of action. In this paper, we have shown that a naturally occurring plant alkaloid, berberine, binds FtsZ and inhibits the Z-ring assembly, thus providing a lead molecule for the development of a new antimicrobial drug. *E. coli* FtsZ used in this study was present as homogeneous linear oligomers in the presence of Mg^{2+} (the aggregates were not present). These could have formed by reversible self-association of monomeric GDP−FtsZ, in agreement with the reported Mg^{2+}-linked noncooperative oligomerization of GDP−FtsZ monomers (*42*).

Berberine exhibits a dose-dependent inhibition of *in vitro* FtsZ assembly kinetics with a concomitant reduction in the

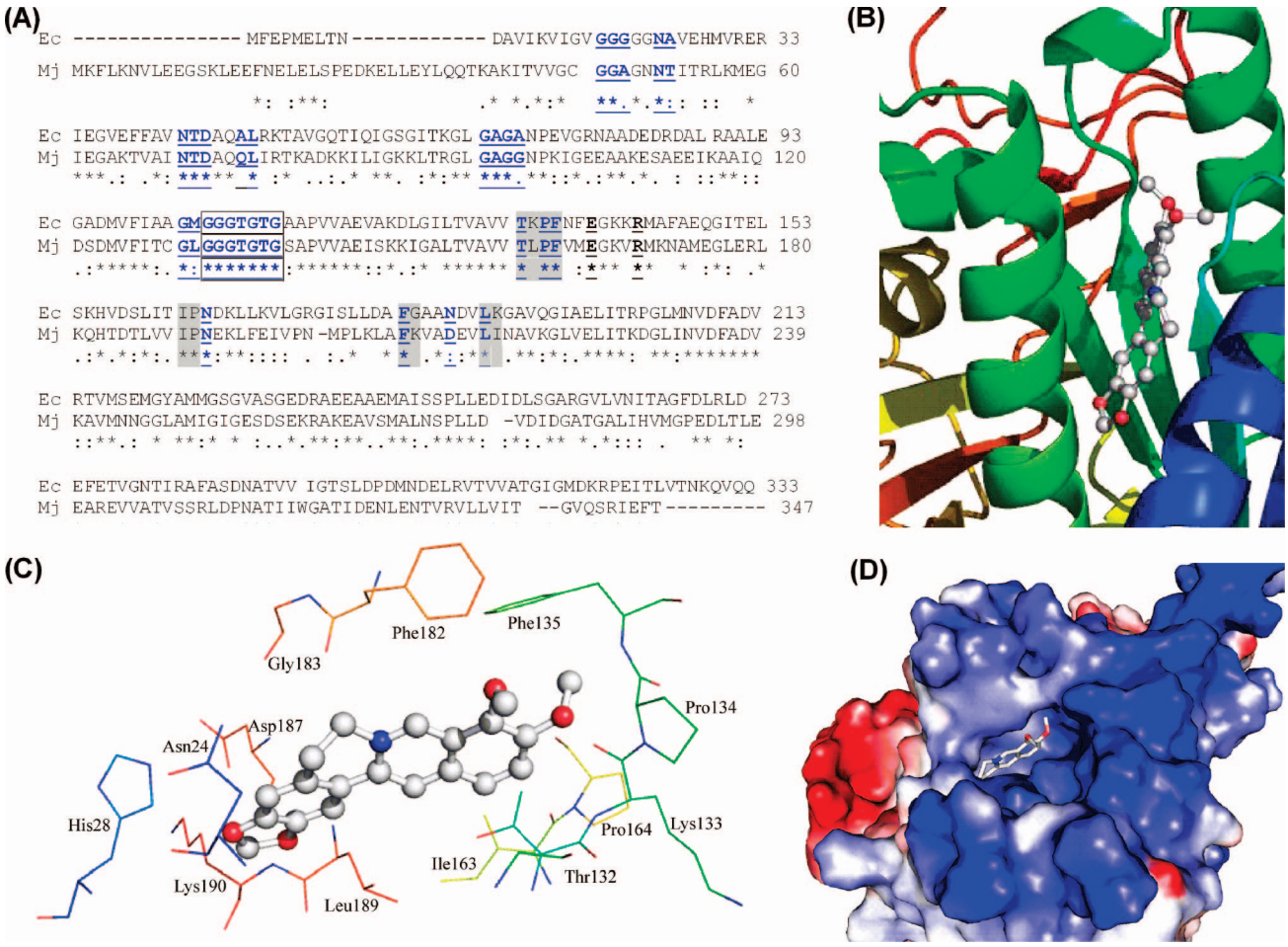

FIGURE 7: Molecular modeling. (A) Sequence alignment of *E. coli* and *M. jannaschii* FtsZ done by CLUSTAL W analysis. Identical residues are shown by asterisks (*), conserved residues are indicated by ":" (more) and "." (less), respectively. Residues highlighted in gray are possibly involved in berberine binding, while residues in bold (underscored) make contact with GDP in FtsZ. The GTP binding motif is boxed. (B) Ribbon diagram showing berberine bound in the GTP binding pocket of the homology model of *E. coli* FtsZ. (C) Close-up view of the active site of berberine on FtsZ. (D) Surface map of berberine in the hydrophobic groove of FtsZ, its blue color intensity being related to its hydrophobic properties.

GTPase activity and binds FtsZ in a 1:1 ratio. In addition, electron microscopy confirmed that berberine destabilizes FtsZ protofilaments, as it causes a reduction in length and bundling of wild-type FtsZ polymers. Since a balanced FtsZ polymer stability is essential for the positional regulation of the Z-ring during the bacterial cell cycle (*43*), we verified if destabilization of FtsZ protofilaments by berberine further affected Z-ring assembly as well. Live cell confocal imaging of GFP-tagged FtsZ showed that berberine equally targeted FtsZ *in vivo* and it inhibited the cellular localization, dynamics, and spatial arrangement of the Z-ring. Berberine prevented the formation of functional Z-rings by blocking the assembly of FtsZ at midcell. Together, the *in vivo* and *in vitro* observations confirmed the role of berberine as a FtsZ inhibitor.

In *E. coli* FtsZ, the GTP binding site (GGGTGTG) is located in the T4 loop between β-sheet S4 and helix H4 (*44*). GTP hydrolysis is activated by the cation-coordinating T7 loop of FtsZ that gets inserted into the GTP binding site of an adjacent monomer (*36*). Earlier, it has been reported that a known FtsZ inhibitor, PC58538, has its binding site located around the edge of the GTP binding pocket and it inhibited the GTPase activity in a dose-dependent manner (*15*). In this study, *in silico* docking placed berberine in the GTP binding hydrophobic pocket of FtsZ. Here, the dose-dependent GTPase inhibition is observed in the presence of berberine. Since GTP hydrolysis is coupled to FtsZ assembly, a decrease in GTP hydrolysis could be a result of the inhibition of the assembly reaction. Further, as FtsZ polymer depletion coincided with GTP exhaustion, it also explained that the inhibition of association of two adjacent FtsZ monomers inhibited its FtsZ GTPase activity. Further, the blue shift (~35 nm) observed upon interaction of berberine to FtsZ indicated that binding resulted as the fluorophoric groups of berberine (aromatic ring and isoquinoline moiety) incorporated into the less polar, hydrophobic milieu of FtsZ. The reduction of FtsZ−bis-ANS fluorescence by berberine suggests that berberine may interfere with binding of bis-ANS to the hydrophobic region of FtsZ. Together, these results imply that the binding of berberine may involve rearrangement of hydrophobic side chains of FtsZ in the GTP binding pocket. Further, the competition experiments of GTP and berberine showed that the fluorescence of FtsZ-bound berberine quenched upon displacement by GTP. It indicated that a few berberine molecules in binding equilibrium with FtsZ also bound to the active (GTPase) pocket of FtsZ, suggesting a probable overlap between binding sites of berberine and GTP. Furthermore, the fluorescence of FtsZ-bound TNP-GTP did not show any obvious change upon sequential additions of increasing concentrations of berberine,

indicating that berberine does not compete with GTP at its binding site. This implies that the binding site of a small molecule like berberine probably lies in the vicinity of the GTP binding pocket of FtsZ, overlapping with a few hydrophobic residues of the active site of FtsZ, viz., Ile 163, Pro 134, Phe 135, Phe 182, and Leu 189, as confirmed by the AutoDock model in conjunction with STD NMR. Although berberine cannot compete with GTP directly, it binds to FtsZ by hydrophobic interactions, overlapping with binding sites of bis-ANS and GTP and inhibits FtsZ self-assembly by inducing rearrangement in the hydrophobic region of FtsZ.

Further, the study of bioenergetics by ITC revealed a thermodynamically favorable reaction, characterized by negative enthalpy and near zero entropy of association. The inflection point of the binding isotherm (near 1.0 molar ratio) indicated that one berberine molecule binds per FtsZ molecule. Binding of berberine to FtsZ was exothermic and involved a near zero entropy change, which suggested the occurrence of a reversible binding process. The Gibbs free energy change predicted that the binding occurs spontaneously, resulting in a favorable interaction between berberine and FtsZ. Since, $\Delta H < 0 < T\Delta S$, the binding process was enthalpy/entropy-driven, favoring a tight binding complexation (*45*) through hydrophobic and hydrogen-bonded specific interactions. The ITC profile also signified a typical pattern for a binding reaction with tight association. The K_D of berberine obtained from ITC data was 0.023 μM. Earlier, the K_D values of bis-ANS (by fluorescence) and GTP (by ITC) were reported to be 1.33 μM (*4*) and 0.003 μM (*46*), respectively. This implies that the affinity of FtsZ for GTP is higher than its affinity for berberine. Berberine is also unable to displace TNP-GTP-bound FtsZ. The K_D of berberine is found to be lower in comparison with bis-ANS, suggesting that berberine probably has a higher affinity to compete with bis-ANS for the same hydrophobic binding pocket. Taken together, the observations from ITC experiments are in agreement with the berberine−bis-ANS fluorescence data (Figure 5B) and the docking simulations (Figure 7), which further supported that berberine probably binds in the hydrophobic region, involving the GTP binding surface of FtsZ.

Furthermore, it may not be appropriate here to correlate the K_D value (obtained by ITC experiment) and the IC_{50} value (obtained by FtsZ assembly kinetics/GTPase assay), as the doses of berberine being assayed are completely different in both experiments in two different buffer conditions for FtsZ. IC_{50} values may not be directly comparable between studies and even between experiments, unless the same ligand and protein preparations have been used and the concentration of the ligand is identical in each assay (*47*). It is also true that the apparent IC_{50} will exceed the actual K_D value for a tight-binding inhibitor when the protein concentration is higher than the K_D value. In this study, berberine has high affinity, with a K_D value of 2×10^{-8} M obtained for a FtsZ concentration of 10×10^{-6} M, indicating that the concentration of berberine required to elicit a half-maximal FtsZ GTPase inhibition (IC_{50}) will exceed its K_D value. In general, it is plausible that the lower the K_D, the greater the difference. Moreover, it is also true that IC_{50} is not a direct indicator of affinity (K_D) although the two can be related only for two competitive ligands by the standard Cheng Prusoff equation (*48*) for binding assay.

Amino acid sequence alignment suggested that certain conserved residues of the GTP binding site of *M. jannaschii* FtsZ (Figure 7A) have common characteristics with the proposed key residues of the berberine binding site of *E. coli* FtsZ, especially Thr 132, Pro 134, Phe 135, Phe 182, and Leu 189. Binding of berberine to any of these residues would result in perturbation of the conformation of the GTP binding pocket and reduction in the GTPase activity of FtsZ, as is also confirmed by our experiments. Hence, the inhibitory role of berberine on the assembly and dynamic behavior of FtsZ polymers can be directly related to the consequential changes in the active conformation of the GTP hydrolysis site.

At an atomic resolution, STD NMR distinguished the functional groups in berberine, which were in close contact with FtsZ. These experiments clearly identified the protons of the dimethoxy groups, the isoquinoline nucleus, and benzodioxolo ring of berberine to be in intimate contact with FtsZ. These observations from STD NMR were also justified by the predicted AutoDock model, which placed berberine in more hydrophobic surface areas surrounding the GTP binding pocket of FtsZ. Together, these results suggested that the hydrophobic residues Pro 134, Phe 135, and Phe 182 were in proximity of one of the dimethoxy groups, 9-OMe (~89% STD NMR effect), suggesting hydrophobic interactions (~1.8 Å). Interestingly, the guanine base of GTP makes hydrophobic contact with a conserved aromatic residue, Phe 182 in *E. coli* FtsZ (*35*), whereas conserved Pro 134 and Phe 135 are involved in the sugar recognition of the bound GDP (*35*). In addition, the protons H10, H11, and H12 (~88% STD NMR effect) of berberine showed closer proximity (~1.8 Å) to the nearby hydrophobic conserved residues like Ile 163 and Pro 164 (*35*) adjacent to Asn 165, which is in contact with GDP in *M. jannaschii* FtsZ (*35*). Moreover, H1, 2-CH_2 protons (~86% STD NMR effect) and H3 protons (~100% STD NMR effect) showed close proximity (~1.8 Å) to Leu 189 (*35*), yet another conserved, hydrophobic residue involved in the base recognition for the bound GDP in *M. jannaschii* FtsZ. The lowest intensities in STD NMR corresponded to H7 and 5-CH_2 (50% STD NMR effect) and indicated that the iminium moiety of berberine was not involved in the binding of berberine to FtsZ (~3.3–3.98 Å). This is in good agreement to the docking model (Figure 7), which showed that the iminium moiety faced the aqueous solution.

In vivo, berberine can readily permeate through the cell membrane of Gram-positive and Gram-negative bacteria (*49*). MIC's of berberine against Gram-negative bacteria such as *E. coli* ATCC 25922, *K. pneumoniae* ATCC 100031, *Proteus vulgaris* ATCC 3851, and *Salmonella typhimurium* ATCC 14028 were reported to be >400 μg/mL, whereas these values are 100 μg/mL for Gram-positive bacteria such as *B. subtilis* ATCC 6633, *Micrococcus luteus* ATCC 9341, and *S. aureus* ATCC 6538p (*50*). MIC's of berberine against methicillin-resistant *S. aureus* (MRSA) were 32−128 μg/mL (*26*), whereas for *Helicobacter pylori*, it was 12.5 μg/mL (*51*). As berberine can inhibit antibiotic-resistant pathogens, it is a prospective model for developing a novel class of antibacterials via targeting FtsZ. A near linear association observed between *E. coli* FtsZ inhibition (IC_{50}) and antibac-

terial activity (MIC for *E. coli*) implies that only a therapeutic and favorable effect is exerted by berberine.

In a recent work, it is shown that, at clinically relevant concentrations, berberine would function more as a mitochondriotropic and cytostatic agent rather than a nuclear-damaging and cytotoxic agent (*52*). Also, it is considered to be nontoxic at doses used in clinical situations, where it shows no genotoxic activity, is unable to induce significant cytotoxic, mutagenic, or recombinogenic effects, and is not a potent mutagenic agent in dividing cells (*53*). Recently, it has been demonstrated that berberine inhibits proliferation and induces G_1-phase arrest and apoptosis in human prostate cancer cells but, interestingly, not in normal human prostate epithelial cells (*54*). It has been found to inhibit apoptosis of thymocytes which are critical immune effector cells. Since, it is a potential chemotherapeutic agent, it is essential that high doses of berberine should not be used without a proper toxicology assessment. Nevertheless, at lower clinically significant doses, it is nontoxic to mammalian cells. Moreover, in order to access for cytotoxicity of berberine in human erythrocytes, we performed a hemolytic assay revealing that berberine is clearly nonhemolytic up to 2 mg/mL (data not shown).

In the literature, there are known inhibitors that bind and inactivate the bacterial cell division protein FtsZ but do not target eukaryotic tubulin (*5, 7, 12*). Berberine is another such FtsZ inhibitor identified here, which does not target mammalian tubulins (*55*). Berberine is similar in function to known FtsZ inhibitors such as PC58538 (*15*) which bind around the GTP binding region on FtsZ and inhibit a broad range of bacteria *in vivo*, in addition of possessing the potential to be developed as antibiotics. In fact, the routine topical or oral use of berberine (Murine, Berberine Plus, Relieva) is already administered in humans, after a number of successful clinical trials (*56–58*). Berberine is excreted through the urine in humans, so it could conceivably have some antibiotic effect in the renal or urinary tract infections (*59*). Hence berberine has the potential to be developed as a lead compound for a novel class of antibiotics via targeting FtsZ. Although berberine has been safely used to treat a number of infections such as eye and trachoma infections, bacterial diarrhea, intestinal tract infections caused by *E. coli*, tuberculosis, cholera, malaria, otitis media, and tumors in humans (*20, 21*), the specific mode of action of berberine was not known. In this paper, we have proposed a novel mechanism of action for berberine, by identifying that berberine targets FtsZ function by binding to its hydrophobic pocket and perturbs Z-ring formation *in vivo*.

ACKNOWLEDGMENT

We thank Prof. H. Mori, Nara Institute of Science and Technology, Japan, for the FtsZ clone, Asst. Prof. S. Bhattacharjya, Nanyang Technological University, Singapore, for the use of NMR spectrometer, and R. Reddy, Michigan University, for help in the modeling. We thank the core facility at the Department of Biological Sciences, National University of Singapore, for electron and confocal microscopy work.

SUPPORTING INFORMATION AVAILABLE

One figure showing berberine displacement assays and one table providing the interproton distances between FtsZ and berberine at the binding site of FtsZ molecules, obtained from the *in silico* docking model. This material is available free of charge via the Internet at http://pubs.acs.org.

REFERENCES

1. Erickson, H. P. (1995) FtsZ, a prokaryotic homolog of tubulin. *Cell 80*, 367–370.
2. Bi, E., and Lutkenhaus, J. (1991) FtsZ ring structure associated with division in *Escherichia coli*. *Nature 354*, 161–164.
3. Margalit, D. N., Romberg, L., Mets, R. B., Hebert, A. M., Mitchison, T. J., Kirschner, M. W., and RayChaudhuri, D. (2004) Targeting cell division: Small-molecule inhibitors of FtsZ GTPase perturb cytokinetic ring assembly and induce bacterial lethality. *Proc. Natl. Acad. Sci. U.S.A. 101*, 11821–11826.
4. Yu, X. C., and Margolin, W. (1998) Inhibition of assembly of bacterial cell division protein FtsZ by the hydrophobic dye 5,5-Bis-(8-anilino-1-naphthalenesulfonate). *J. Biol. Chem. 273*, 10216–10222.
5. Wang, J., Galgoci, A., Kodali, S., Herath, K. B., Jayasuriya, H., Dorso, K., Vicente, F., Gonzalez, A., Cully, D., Bramhill, D., and Singh, S. (2003) Discovery of a small molecule that inhibits cell division by blocking FtsZ, a novel therapeutic target of antibiotics. *J. Biol. Chem. 278*, 44424–44428.
6. Urgaonkar, S., La Pierre, H. S., Meir, I., Lund, H., RayChaudhuri, D., and Shaw, J. T. (2005) Synthesis of antimicrobial natural products targeting FtsZ: (+/−)-dichamanetin and (+/−)-2′ ″-hydroxy-5″-benzylisouvarinol-B. *Org. Lett. 7*, 5609–5612.
7. Jaiswal, R., Beuria, T. K., Mohan, R., Mahajan, S. K., and Panda, D. (2007) Totarol Inhibits Bacterial Cytokinesis by Perturbing the Assembly Dynamics of FtsZ. *Biochemistry 46*, 4211–4220.
8. Beuria, T. K., Santra, M. K., and Panda, D. (2005) Sanguinarine Blocks Cytokinesis in Bacteria by Inhibiting FtsZ Assembly and Bundling. *Biochemistry 44*, 16584–16593.
9. Domadia, P., Swarup, S., Bhunia, A., Sivaraman, J., and Dasgupta, D. (2007) Inhibition of bacterial cell division protein FtsZ by cinnamaldehyde. *Biochem. Pharmacol. 74*, 831–840.
10. White, E. L., Suling, W. J., Ross, L. J., Seitz, L. E., and Reynolds, R. C. (2002) 2-Alkoxycarbonyl aminopyridines: inhibitors of *Mycobacterium tuberculosis* FtsZ. *J. Antimicrob. Chemother. 50*, 111–114.
11. Huang, Q., Tonge, P. J., Slayden, R. A., Kirikae, T., and Ojima, I. (2007) FtsZ: a novel target for tuberculosis drug discovery. *Curr. Top. Med. Chem. 7*, 527–543.
12. Lappchen, L. T., Hartog, A. F., Pinas, V. A., Koomen, G. J., and den Blaauwen, T. (2005) GTP analogue inhibits polymerization and GTPase activity of the bacterial protein FtsZ without affecting its eukaryotic homologue tubulin. *Biochemistry 44*, 7879–7884.
13. Catherine, P. B., Beaumont, M., Sanschagrin, F., Voyer, N., and Levesque, R. C. (2007) Parallel solid synthesis of inhibitors of the essential cell division FtsZ enzyme as a new potential class of antibacterials. *Bioorg. Med. Chem. Lett. 15*, 1330–1340.
14. Ito, H., Ura, A., Oyamada, Y., Tanitame, A., Yoshida, H., Yamada, S., Wachi, M., and Yamagishi, J. (2006) A 4-aminofurazan derivative-A189-inhibits assembly of bacterial cell division protein FtsZ in vitro and in vivo. *Microbiol. Immunol. 50*, 759–764.
15. Stokes, N. R., Sievers, J., Barker, S., Bennett, J. M., Brown, D. R., Collins, I., Errington, V. M., Foulger, D., Hall, M., Halsey, R., Johnson, H., Rose, V., Thomaides, H. B., Haydon, D. J., Czaplewski, L. G., and Errington, J. (2005) Novel inhibitors of bacterial cytokinesis identified by a cell-based antibiotic screening assay. *J. Biol. Chem. 280*, 39709–39715.
16. Reynolds, R. C., Srivastava, S., Ross, L. J., Suling, W. J., and White, E. L. (2004) A new 2-carbamoyl pteridine that inhibits mycobacterial FtsZ. *Bioorg. Med. Chem. Lett. 14*, 3161–3164.
17. Huang, Q., Kirikae, F., Kirikae, T., Pepe, A., Amin, A., Respicio, L., Slayden, R. A., Tonge, P. J., and Ojima, I. (2006) Targeting FtsZ for antituberculosis drug discovery: Noncytotoxic taxanes as novel antituberculosis agents. *J. Med. Chem. 49*, 463–466.
18. Kong, D. X., Li, X. J., Tang, G. Y., and Zhang, H. Y. (2007) How Many Traditional Chinese Medicine Components Have Been Recognized by Modern Western Medicine? A Chemoinformatic Analysis and Implications for Finding Multicomponent Drugs. *ChemMedChem* (in press).
19. Amin, A. H., Subbaiah, T. V., and Abbasi, K. M. (1969) Berberine sulfate: antimicrobial activity, bioassay, and mode of action. *Can. J. Microbiol. 15*, 1067–1076.

20. Timothy, C., Birdsall, N. D., Gregory, S., and Kelly, N. D. (1997) Berberine: Therapeutic Potential of an Alkaloid Found in Several Medicinal Plants. *Altern. Med. Rev. 2*, 94–103.
21. Anonymous. (2000) Berberine monograph. *Altern. Med. Rev. 5*, 175–177.
22. Rees, L. P., Minney, S. F., Plummer, N. T., Slater, J. H., and Skyrme, D. A. (1993) A quantitative assessment of the antimicrobial activity of garlic (*Allium sativum*). *World J. Micrbiol. Biotechnol. 9*, 303–307.
23. Hwang, B. Y., Roberts, S. K., Chadwick, L. R., Wu, C. D., and Kinghorn, A. D. (2003) Antimicrobial constituents from goldenseal (the rhizomes of *Hydrastis canadensis*) against selected oral pathogens. *Planta Med. 69*, 623–627.
24. Villinski, J. R., Dumas, E. R., Chai, H., Pezzuto, J. M., Angerhofer, C. K., and Gafner, S. (2003) Antibacterial Activity and Alkaloid Content of *Berberis thunbergii*, *Berberis vulgaris* and *Hydrastis canadensis*. *Pharm. Biol. 41*, 551–557.
25. Gentry, E. J., Jampani, H. B., Keshavarz-Shokri, A., Morton, M. D., Velde, D. V., Telikepalli, H, Mitscher, L. A., Shawar, R., Humble, D., and Baker, W. (1998) Antitubercular natural products: berberine from the roots of commercial *Hydrastis canadensis* powder. Isolation of inactive 8oxotetrahydrothalifendine, canadine, beta-hydrastine, and two new quinic acid esters, hycandinic acid esters-1 and -2. *J. Nat. Prod. 61*, 1187–1193.
26. Yu, H., Kim, K., Cha, J., Kim, H., Lee, Y., Choi, N., and You, Y. (2005) Antimicrobial activity of berberine alone and in combination with ampicillin or oxacillin against methicillin-resistant *Staphylococcus aureus*. *J. Med. Food 8*, 454–461.
27. Kitagawa, M., Ara, T., Arifuzzaman, M., Nakamichi, T., Inamoto, E., Toyonaga, H., and Mori, H. (2005) Complete set of ORF clones of *Escherichia coli* ASKA library (A Complete Set of *E. coli* K-12 ORF Archive): Unique Resources for Biological Research. *DNA Res. 12*, 291–299.
28. Mukherjee, A., and Lutkenhaus, J. (1999) Analysis of FtsZ assembly by light scattering and determination of the role of divalent metal cations. *J. Bacteriol. 181*, 823–832.
29. Geladopoulos, T. P., Sotiroudis, T. G., and Evangelopoulos, A. E. (1991) A malachite green colorimetric assay for protein phosphatase activity. *Anal. Biochem. 192*, 112–116.
30. Mayer, M., and Meyer, B. (2001) Group Epitope Mapping by Saturation Transfer Difference NMR to identify Segments of a Ligand in Direct Contact with a Protein Receptor. *J. Am. Chem. Soc. 123*, 6108–6117.
31. Meyer, B., and Peters, T. (2003) NMR spectroscopy techniques for screening and identifying ligand binding to protein receptors. *Angew. Chem., Int. Ed. 42*, 864–890.
32. Radda, G. K. (1973) in *Fluorescence Techniques in Cell Biology* (Thaer, A. A., and Sernetz, M., Eds.) pp 261–272, Springer-Verlag, Berlin, Heidelberg, and New York.
33. Hiratsuka, T. (2003) Fluorescent and colored trinitrophenylated analogs of ATP and GTP. *Eur. J. Biochem. 270*, 3479–3485.
34. Morris, G. M., Goodsell, D. S., Halliday, R. S., Huey, R., Hart, W. E., Belew, R. K., and Olson, A. J. (1998) Automated docking using a Lamarckian genetic algorithm and empirical binding free energy function. *J. Comput. Chem. 19*, 1639–1662.
35. Lowe, J., and Amos, L. A. (1998) Crystal structure of the bacterial cell-division protein FtsZ. *Nature 391*, 203–206.
36. Scheffers, D. J., de Wit, J. G., den Blaauwen, T., and Driessen, A. J. M. (2002) GTP hydrolysis of cell division protein FtsZ: Evidence that the active site is formed by the association of monomers. *Biochemistry 41*, 521–529.
37. Marquardt, D. W. (1963) An algorithm for least squares estimation of nonlinear parameters. *J. Soc. Ind. Appl. Math. 11*, 431–441.
38. Maiti, M., and Suresh Kumar, G. (2007) Molecular aspects on the interaction of protoberberine, benzophenanthridine and aristolochia group of alkaloids with nucleic acid structures and biological perspectives. *Med. Res. Rev. 27*, 649–695.
39. Rosen, C. G., and Weber, G. (1969) Dimer formation from 1-anilino-8-naphthalene sulfonate catalyzed by bovine serum albumin—A new fluorescent molecule with exceptional binding properties. *Biochemistry 8*, 3915–3920.
40. Mukherjee, A., Santra, M. K., Beuria, T. K., and Panda, D. (2005) A natural osmolyte trimethylamine N-oxide promotes assembly and bundling of the bacterial cell division protein, FtsZ and counteracts the denaturing effects of urea. *FEBS J. 272*, 2760–2772.
41. Tsien, R. Y. (1998) The green fluorescence protein. *Annu. Rev. Biochem. 67*, 509–544.
42. Rivas, G., López, A., Mingorance, J., Ferrándiz, M. J., Zorrilla, S., Minton, A. P., Vicente, M., and Andreu, J. M. (2000) Magnesium-induced linear self-association of the FtsZ bacterial cell division protein monomer. The primary steps for FtsZ assembly. *J. Biol. Chem. 275*, 11740–11749.
43. Levin, P. A., Schwartz, R. L., and Grossman, A. D. (2001) Polymer stability plays an important role in the positional regulation of FtsZ. *J. Bacteriol. 183*, 5449–5452.
44. Nogales, E., Downing, K. H., Amos, L. A., and Löwe, J. (1998) Tubulin and FtsZ form a distinct family of GTPases. *Nat. Struct. Biol. 5*, 451–458.
45. Gilli, P., Gilli, G., Borea, P. A., Varani, K., Scatturin, A., and Dalpiaz, A. (2005) Binding Thermodynamics as a Tool To Investigate the Mechanisms of Drug-Receptor Interactions: Thermodynamics of Cytoplasmic Steroid/Nuclear Receptors in Comparison with Membrane Receptors. *J. Med. Chem. 48*, 2026–2035.
46. Huecas, S., Schaffner-Barbero, C., García, W., Yébenes, H., Palacios, J. M., Díaz, J. F., Menéndez, M., and Andreu, J. M. (2007) The interactions of cell division protein FtsZ with guanine nucleotides. *J. Biol. Chem. 282*, 37515–37528.
47. Orchinik, M., and Propper, C. R. (2005) Hormone action on receptors, in *Introduction to Endocrinology* (Norris, D. O., and Carr, J. A., Eds.) Oxford University Press, New York.
48. Cheng, Y., and Prusoff, W. H. (1973) Relationship between the inhibition constant (K1) and the concentration of inhibitor which causes 50% inhibition (I50) of an enzymatic reaction. *Biochem. Pharmacol. 22*, 3099–3108.
49. Severina, I. I., Muntyan, M. S., Lewis, K., and Skulachev, V. P. (2001) Transfer of cationic antibacterial agents berberine, palmatine and benzalkonium through bimolecular planar phospholipid film and *Staphylococcus aureus* membrane. *IUBMB Life Sci. 52*, 321–324.
50. Kim, S. H., Shin, D. S., Oh, M. N., Chung, S. C., Lee, J. S., and Oh, K. B. (2004) Inhibition of the bacterial surface protein anchoring transpeptidase sortase by isoquinoline alkaloids. *Biosci., Biotechnol., Biochem. 68*, 421–424.
51. Mahady, G. B., Pendland, S. L., Stoia, A., and Chadwick, L. R. (2003) In Vitro Susceptibility of *Helicobacter pylorito* Isoquinoline Alkaloids from *Sanguinaria canadensis* and *Hydrastis canadensis*. *Phytother. Res. 17*, 217–221.
52. Serafim, T. L., Oliveira, P. J., Sardao, V. A., Perkins, E., Parke, D., and Holy, J. (2007) Different concentrations of berberine result in distinct cellular localization patterns and cell cycle effects in a melanoma cell line. *Cancer Chemother. Pharmacol.* (in press).
53. Pasqual, M. S., Lauer, C. P., Moyna, P., and Henriques, J. A. (1993) Genotoxicity of the isoquinoline alkaloid berberine in prokaryotic and eukaryotic organisms. *Mutat. Res. 286*, 243–252.
54. Mantena, S. K., Sharma, S. D., and Katiyar, S. K. (2006) Berberine, a natural product, induces G1-phase cell cycle arrest and caspase-3dependent apoptosis in human prostate carcinoma cells. *Mol. Cancer Ther. 5*, 296–308.
55. Ho, J., and Fishwild, D. M. (2004) Screening cytoactive compounds to determine cell cycle arrest using the Guava PCA−96 System, a microplate based benchtop cell analysis system,Guava Technologies Inc.
56. Kong, W., Wei, J., Abidi, P., Lin, M., Inaba, S., Li, C., Wang, Y., Wang, Z., Si, S., Pan, H., Wang, S., Wu, J., Wang, Y., Li, Z., Liu, L., and Jiang, J. D. (2004) Berberine is a novel cholesterol-lowering drug working through a unique mechanism distinct from statins. *Nat. Med. 10*, 1344–1351.
57. Babbar, O. P., Chhatwal, V. K., Ray, I. B., and Mehra, M. K. (1982) Effect of berberine chloride eye drops on clinically positive trachoma patients. *Ind. J. Med. Res. 76*, 83–88.
58. Rabbani, G. H., Butler, T., Knight, J., Sanyal, S. C., and Alam, K. (1987) Randomized controlled trial of berberine sulfate therapy for diarrhea due to enterotoxigenic *E. coli* and *Vibrio cholerae*. *J. Infect. Dis. 155*, 979–984.
59. Pan, J. F., Yu, C., Zhu, D. Y., Zhang, H., Zeng, J. F., Jiang, S. H., and Ren, J. Y. (2002) Identification of three sulfate-conjugated metabolites of berberine chloride in healthy volunteers' urine after oral administration. *Acta Pharmacol. Sin. 23*, 77–82.

BI7018546